

## Nanoparticles of Cobalt Ferrite for NH<sub>3</sub> Sensing

<sup>1</sup> Christine LEROUX, <sup>2</sup> Marc BENDAHAN, <sup>1</sup> Véronique MADIGOU,  
<sup>3</sup> Lilia AJROUDI, <sup>3</sup> Najeh MLIKI

<sup>1</sup> Université Sud Toulon Var, IM2NP UMR CNRS 7334, BP20132, 83957 La Garde Cedex, France

<sup>2</sup> Aix Marseille Université, IM2NP UMR CNRS 7334, Av. Escadrille Normandie Niemen,  
case 152, 13397 Marseille Cedex, France

<sup>3</sup> LMOP, Faculté des Sciences de Tunis, Université Tunis El Manar, 2090 Tunis, Tunisie

<sup>1</sup> Tel.: +33 (0) 494142312, fax: +33 (0) 494142168

E-mail: leroux@univ-tln.fr

Received: 23 November 2013 / Accepted: 12 January 2014 / Published: 26 May 2014

**Abstract:** The electrical response of cobalt ferrites Co<sub>x</sub>Fe<sub>3-x</sub>O<sub>4</sub> nanopowders was tested in presence of ammonia. The morphology, shape and chemical composition of the powder was fully characterized by transmission electron microscopy. Fast response, good sensitivity and good reversibility were evidenced, with detection even at 5 ppm NH<sub>3</sub>. Gas selectivity depends on the cobalt amount, x, in cobalt ferrite powders. Copyright © 2014 IFSA Publishing, S. L.

**Keywords:** Cobalt ferrites, NH<sub>3</sub> sensor, Nanoparticles.

### 1. Introduction

Research devoted to the use of ferrites for gas sensing and pollution monitoring increased abruptly in the last 10 years [1-2]. The main reason for that is the capability of fine tuning of electrical properties in these semi-conductor compounds; depending on the cation composition, ferrites will exhibit n or p type conductivity. Ferrites can also have oxygen vacancies, which again modify the conduction properties, hence the electrical response of the sensor [3]. Among ferrites, cubic spinel like CuFe<sub>2</sub>O<sub>4</sub> [4], or MgFe<sub>2</sub>O<sub>4</sub> [5] showed fast time responses and temperature controlled selectivity. There are many fields in human activity where there is a need to detect and measure ammonia, but the limit of detection, the time response and the working temperature vary. For medical applications, the detected ammonia concentration should be of the order of some ppb, but a fast response is not needed, as for air quality control, fast response are needed, for concentrations

in the range of the 10-20 ppm [6]. Cubic spinel ferrite proved to be potential new sensing materials for ammonia. Thick films of nickel ferrite showed good sensitivity to ammonia at room temperature [7]. Mixed cobalt and nickel ferrites were synthesized as nanoparticles and the sensitivity towards ammonia was better for low nickel content [8].

In this work, we tested the capability of cobalt ferrites nanoparticles, synthesized by a solvo thermal method, to detect low concentrations of NH<sub>3</sub>, as well as the time response. The catalytic behavior of these nanoparticles in presence of reducing gases was already evidenced [9]. Several compositions were synthesized, among them x=1.8 and x=1. The catalytic efficiency depends on the cobalt amount x in Co<sub>x</sub>Fe<sub>3-x</sub>O<sub>4</sub>, and the best one was obtained for x=1.8. Thus, cobalt ferrite with this concentration was mainly tested. In literature cobalt ferrite often refers to Co<sub>1</sub>Fe<sub>2</sub>O<sub>4</sub>, therefore cobalt ferrite with x=1 was also investigated in this study.

## 2. Experimental

Cobalt (II) 2,4-pentanedionate and iron (III) acetylacetonate, were dissolved in benzyl alcohol. The solution was poured into a teflon cup, which was sealed into a steel autoclave, and heated in a furnace at 175 °C for 48 hours. Details can be found in a previous article [9]. Cobalt ferrites with several concentrations were synthesized, among them  $x=1.8$ , which is the composition studied in this work. High resolution electron microscopy (HREM) coupled with Energy Dispersive Spectroscopy (EDS) and X rays diffraction were used to characterize the powders at a sub-nanometer scale. Fig. 1 shows well crystallized nanoparticles of  $\text{Co}_x\text{Fe}_{3-x}\text{O}_4$  with  $x=1.8$ . The individual Fast Fourier Transform of the HREM images could all be indexed in the spinel structure, confirming the X-Rays diffraction results about a single phased powder with spinel structure [9]. EDS analyses showed a weak dispersion in composition ( $x=1.76 \pm 0.04$ ). The mean size of the particles is 4 nm (see histogram Fig. 1). For  $x=1$ , the particles are more spherical, with a mean size of 6.5 nm [10].

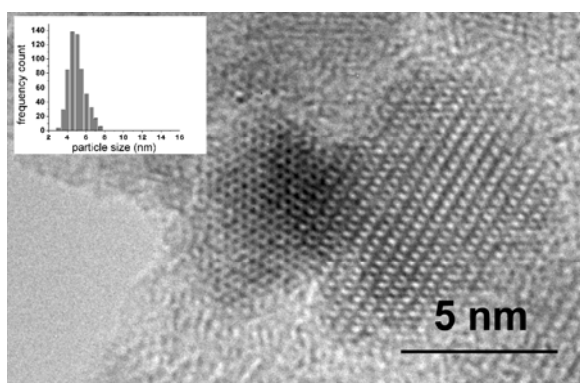


**Fig. 1.** HREM images of  $\text{Co}_{1.8}\text{Fe}_{1.2}\text{O}_4$  particles, along with the size distribution over 500 particles. The particles are well crystallized and exhibit very irregular shapes.

The powder were dispersed in terpineol and deposited by solution drop casting on  $\text{SiO}_2/\text{Si}$  substrates with platinum electrodes, followed by a heating at 300 °C. A previous study showed that the particle size remains the same for such low temperature treatment [10]. As  $\text{Co}_x\text{Fe}_{3-x}\text{O}_4$  layers are highly resistive, interdigitated electrodes were used in order to reduce the sensor resistance. The distance between the electrodes was 50  $\mu\text{m}$ . They were obtained from a sputtered Pt film, using photolithography and lift off processes. A very thin titanium layer is deposited before the platinum layer to enhance the adhesion on  $\text{SiO}_2/\text{Si}$  substrates. Fig. 2 shows the porous covering of the substrate by the powder.

The samples were kept in dry air and no conditioning step was carried out before the sensor characterizations. To investigate the  $\text{NH}_3$  sensing properties of the  $\text{Co}_x\text{Fe}_{3-x}\text{O}_4$  films, the sensor devices

are introduced in a test chamber allowing the sensor temperature control under variable gas concentrations. Dry synthetic air was used as a reference gas and as a diluting gas to obtain the desired concentrations. The sensor performances were tested at atmospheric pressure. The baseline sensor resistance was stabilized in dry air at the selected operating temperature. The gas flows were measured through mass flow-meters and the studied concentrations ranged from 5 to 100 ppm with a constant total flow of 0.2 l/min. The electrical sensor resistance was acquired by means of a sourcemeter (Keithley 2400). Fig. 3 shows the experimental set up for electrical measurements.

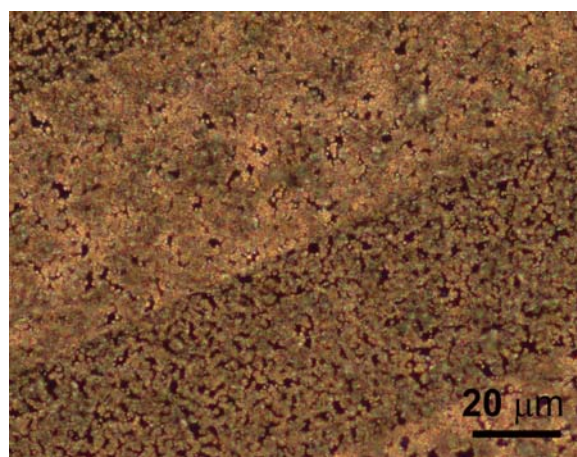


**Fig. 2.** Optical micrograph after drop casting showing the covering between the electrodes (darker part of the image) and on top of the electrodes (lighter part of the image).

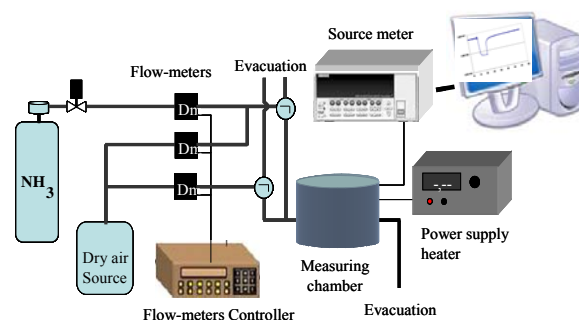


**Fig. 3.** Experimental set-up for gas sensitivity studies.

The sensitivity of the sensor was defined as  $S = R_{\text{gas}}/R_{\text{air}}$  for a p-type semi conductor and  $S = R_{\text{air}}/R_{\text{gas}}$  for an n-type semi conductor, with  $R_{\text{air}}$  and  $R_{\text{gas}}$  being the sensor resistances under dry air and under (dry air +  $\text{NH}_3$ ), respectively. The detection time  $\tau_d$  is defined as the time necessary to reach 90 % of the resistance under gas when exposing the sensor to ammonia. The recovery time  $\tau_r$  is defined as the time necessary to reach 90 % of the resistance under dry air, after stopping ammonia flux.

### 3. NH<sub>3</sub> Sensing

#### 3.1. Sensor Based on Co<sub>x</sub>Fe<sub>3-x</sub>O<sub>4</sub> with x = 1.8

Semi conductor sensors are known to have an optimum working temperature, in terms of sensitivity [11-12]. This optimum working temperature was already determined in a previous study [13]. Fig. 4 illustrates the sensitivity of the sensor exposed to 40 ppm of ammonia versus operating temperature. It shows a systematic increase of response with increasing operating temperature below 500 K, but reversal tendency is observed above 500 K. This behavior can be explained by considering the temperature dependence of the surface coverage of chemisorbed species. At low temperature, the desorption rate is weak and a total surface coverage can be obtained. At high temperature, the desorption rate is faster than the adsorption rate and the coverage decreases with increasing temperature. In between these two regimes there is an optimum temperature corresponding to the maximum sensitivity of the sensor. The best response is measured at 500 K. However, the response  $\tau_d$  and  $\tau_r$  recovery times have also to be taken into account. They are related to the adsorption and desorption activation energies. At 500 K, sensitivity is high, but recovery time too long (more than 2 minutes at 50 ppm). At 530 K desorption is faster and the recovery time is short enough (see table 1) but the sensitivity is lower. At 573 K, the recovery time is as fast as the detection time ( $t = 5s$ ) for 25 ppm, but the sensitivity is too low at this temperature. Thus, the best compromise between a good sensitivity and fast recovery time corresponds to a working temperature of 530 K. For this temperature, the detection time of the sensor is short, between 7 and 10 seconds (see table 1). The detection time does not depend on the NH<sub>3</sub> concentration; this is easily explained by the fact that the sensor is sensible to very low concentration of NH<sub>3</sub>. The recovery time is dependent on NH<sub>3</sub> concentration; for high concentration, more time is necessary to regenerate the high amount of adsorbed gas molecules. The recovery time is also shorter at higher temperature, because of higher desorption rates.

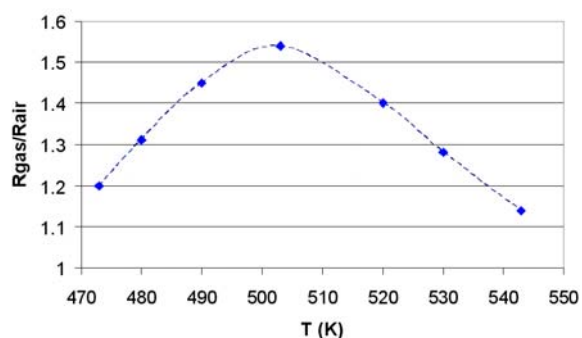


Fig. 4. Sensitivity of the cobalt ferrite sensor versus operating temperature.

Table 1. Detection  $\tau_d$  (s) and recovery  $\tau_r$  (s) times at two temperatures, for various NH<sub>3</sub> concentrations.

	NH <sub>3</sub> [ppm]	100	50	25	10
T=533 K	$\tau_d$ (s)	7	8	10	9
	$\tau_r$ (s)	57	40	37	22
T=573 K	$\tau_d$ (s)	4	4.5	5	
	$\tau_r$ (s)	11	8	6	

In order to study the sensitivity to low ammonia concentration, the sensor was heated at 530 K and exposed to ammonia concentrations between 5 and 100 ppm. Fig. 5 shows good sensitivity even a very low NH<sub>3</sub> concentration ( $R_{\text{gas}}/R_{\text{air}}=1.4$  for 5 ppm). From this curve, one can even expect sensitivity at 2 ppm.

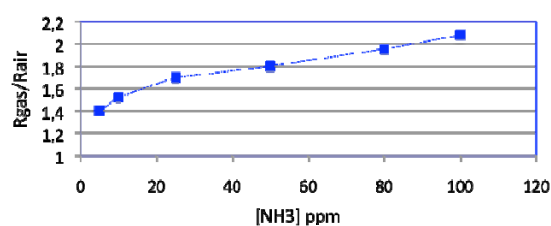


Fig. 5. Sensitivity of the cobalt ferrite sensor versus NH<sub>3</sub> concentration at 530 K.

Baseline stability, response reversibility, and response reproducibility are also very important parameters for evaluating sensor performances. In Fig. 6, we have recorded three sensor response cycles of the device exposed to 10 ppm, 25 ppm and 50 ppm for 35 s at 530 K. Fig. 6 shows the good short term reproducibility of the sensor response. Reproducibility tests over one week showed a weak decrease in the sensor response. Further investigations are needed to understand this phenomenon. We can notice that this sensor exhibits attractive performances: good response to low NH<sub>3</sub> concentrations, reversibility, reproducibility, and baseline stability. Co<sub>1.8</sub>Fe<sub>1.2</sub>O<sub>4</sub> resistance increases in presence of ammonia, which means that this cobalt ferrite is a p-type semi conductor.

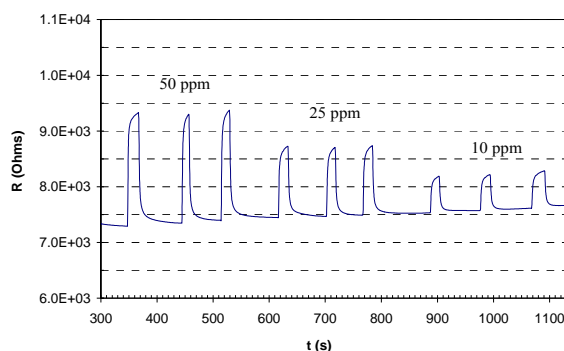


Fig. 6. Sensor response repeatability for Co<sub>x</sub>Fe<sub>3-x</sub>O<sub>4</sub> with x = 1.8 (T = 530 K).

### 3.2 Sensor based on $\text{Co}_x\text{Fe}_{3-x}\text{O}_4$ with $x = 1$

In order to investigate the importance of composition in cobalt ferrites sensing properties, sensors with  $x=1$  were also prepared. In Fig. 7 we have represented the sensor response for 50 ppm, 100 ppm and 200 ppm of  $\text{NH}_3$ . The sensor response is completely different from the sensor with  $x = 1.8$ . The sensitivity is weak even for high amount (200 ppm) of  $\text{NH}_3$  and the resistance decreases in ammonia presence (reducing gas).  $\text{CoFe}_2\text{O}_4$  has an n-type semiconductor behaviour, in opposition to the compound with  $x = 1.8$ , which is a p-type semiconductor.

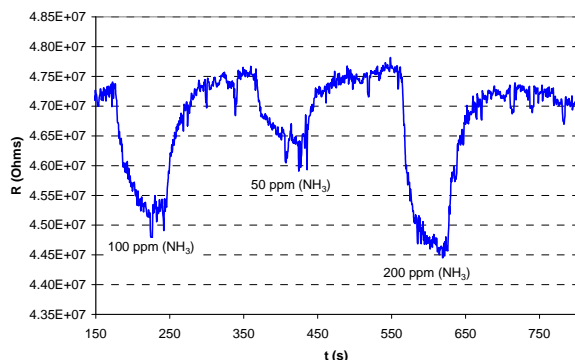
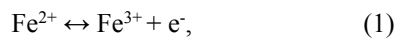


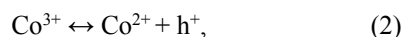
Fig. 7. Sensor response for  $\text{Co}_x\text{Fe}_{3-x}\text{O}_4$  with  $x = 1$  at 523 K.

### 4. Discussion

Conductivity in ferrites is explained in terms of small polaron hopping between cations on octahedral sites [14]. In the cobalt ferrite spinels, the cation distribution on tetrahedral sites A and octahedral sites B structure varies. In case of magnetite  $\text{Fe}_3\text{O}_4$  ( $x=0$ ), one has a so called inverse spinel, with the cation distribution being  $[\text{Fe}^{3+}]_A [\text{Fe}^{2+}\text{Fe}^{3+}]_B\text{O}_4$ .  $\text{Fe}_3\text{O}_4$  is an n-type semiconductor, according to the equation:



In case of cobaltite  $\text{Co}_3\text{O}_4$  ( $x=3$ ), one has a normal spinel, with a cation distribution  $[\text{Co}^{2+}]_A [\text{Co}^{3+}]_B\text{O}_4$ .  $\text{Co}_3\text{O}_4$  is a p-type semiconductor, according to the equation:



For cobalt ferrite, depending on the cobalt amount and the preparation method, the conductivity will be of n or p type [15]. Our measurements indicate that most probably, for  $x=1.8$ ,  $\text{Co}^{3+}$  cations are present on octahedral sites. The difference in sensitivity between the sensor with  $x=1$  and the one with  $x=1.8$  can be related to a difference in conductivity (transduction function) or to a difference in detection mechanism. Studies about intergrain conductivity in nanopowders

of  $\text{Co}_x\text{Fe}_{3-x}\text{O}_4$  showed similar conductivities values for  $x=1$  and  $x=1.8$  [16]. This indicates that the difference in sensitivity to  $\text{NH}_3$  of these two compounds is not linked to the transduction function of the compounds. Holes in p-type semiconductors are known to favour surface oxygen mobility and oxygen chemisorption [17]. The high sensitivity of  $x=1.8$  could also be related to the irregular shape of the particles, and to their smaller sizes, leading to more active sites able to adsorb oxygen under air.

### 5. Conclusions

In automotive industry, the air quality in passenger cabinet requires time responses of the order of one second for  $\text{NH}_3$  concentrations below 50 ppm, and the control of  $\text{NH}_3$  in exhaust gases requires a sensing material reacting in seconds at concentration below 10 ppm, and working at temperatures around 300 °C. Good sensitivity at low  $\text{NH}_3$  concentration (5-10 ppm) as well as fast detection times (5-10s) makes cobalt ferrite  $\text{Co}_x\text{Fe}_{3-x}\text{O}_4$  (with  $x$  near 2) a good sensing material for indoor air quality monitoring.

### Acknowledgements

Authors acknowledge the PHC-Utique French Tunisian exchange program 11G 1301 for financial support.

### References

- [1]. A. Virden, S. Wells, K. O'Grady, Physical and magnetic properties of highly anisotropic cobalt ferrite particles, *Journal of Magnetism and Magnetic Materials*, 316, 2007, pp. 768-771
- [2]. D. S. Mathew, R. S. Juang, An overview of the structure and magnetism of spinel ferrite nanoparticles and their synthesis in microemulsions, *Chemical Engineering Journal*, 129, 2007, pp. 51-65.
- [3]. A. Sutka, G. Mezinskis, A. Lulis, M. Stingaciuc, Influence of iron non-stoichiometry on spinel zinc ferrite gas sensing properties, *Sensors and Actuators B*, 171-172, 2012, pp. 354-360.
- [4]. Z. Sun, L. Liu, D. Z. Jia, W. Pan, Simple synthesis of  $\text{CuFe}_2\text{O}_4$  nanoparticles as gas sensing materials, *Sensors and Actuators B*, 125, 2007, pp. 144-148.
- [5]. Y.-L. Liu, Z.-M. Liu, Y. Yang, H.-F. Yang, G.-L. Shen, R.-Q. Yu, Simple synthesis of  $\text{MgFe}_2\text{O}_4$  nanoparticles as gas sensing materials, *Sensors and Actuators B*, 107, 2005, pp. 600-604.
- [6]. B. Timmer, W. Olthuis, A. van den Berg, Ammonia sensors and their applications - a review, *Sensors and Actuators B*, 107, 2005, pp. 666-677.
- [7]. R. B. Kamble, V. L. Mathe, Nanocrystalline nickel ferrite thick film as an efficient gas sensor at room temperature, *Sensors and Actuators B*, 131, 2008, pp. 205-209.
- [8]. Y. Tang, X. W. Wang, Q. H. Zhang, Y. G. Li, H. Z. Wang, Solvothermal synthesis of  $\text{Co}_{1-x}\text{Ni}_x\text{Fe}_2\text{O}_4$

- nanoparticles and its application in ammonia vapors detection, *Progress in Natural Sciences-Materials International*, 22, 2012, pp. 53-58.
- [9]. L. Ajroudi, V. Madigou, S. Villain, N. Mliki, Ch. Leroux, Synthesis and microstructure of cobalt ferrite nanoparticles, *Journal of Crystal Growth*, 312, 2010, pp. 2465-2471.
- [10]. L. Ajroudi, V. Madigou, S. Villain, N. Mliki, Ch. Leroux Potentiality of cobalt nanoferrites for gas sensors, *Sensor Letters*, 9, 2011, pp. 1-4.
- [11]. M. Bendahan, R. Boulmani, J. L. Seguin, K. Aguir, Characterization of ozone sensors based on WO<sub>3</sub> reactively sputtered films: influence of O<sub>2</sub> concentration in the sputtering gas, and working temperature, *Sensors and Actuators B*, 100, 2004, pp. 320-324.
- [12]. J. Guérin, M. Bendahan, K. Aguir, A dynamic response model for the WO<sub>3</sub>-based ozone sensors, *Sensors and Actuators B*, 128, 2008, pp. 462-467.
- [13]. Ch. Leroux, M. Bendahan, L. Ajroudi, V. Madigou, N. Mliki, Cobalt Ferrite, a New Gas Sensing Material, in *Proceedings of the IMCS'12 Conference*, 2012, pp. 1119 - 1121.
- [14]. D. Emin, N. L. Huang. Liu, Small polaron hopping in magnetic semiconductors, *Physical Review B*, 27, 1983, pp. 4788-4798.
- [15]. C. Xiangfeng, J. Dongli, G. Yu, Z. Chenmou, Ethanol gas sensor based on CoFe<sub>2</sub>O<sub>4</sub> nano-crystalline prepared by hydrothermal method, *Sensors and Actuators B*, 120, 2006, pp. 177-181.
- [16]. L. Ajroudi, V. Madigou, L. Bessais, S. Villain, N. Mliki, Ch. Leroux, 2013, to be submitted to *Acta Materialia*.
- [17]. G. Korotcenkov, Metal oxides for solid-state gas sensors: What determines our choice ?, *Materials Science and Engineering B*, 139, 2007, pp.1-23.

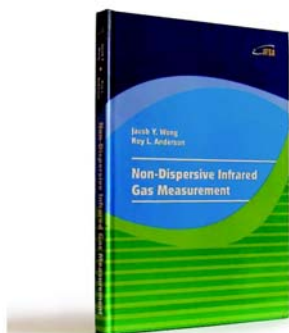
2014 Copyright ©, International Frequency Sensor Association (IFSA) Publishing, S. L. All rights reserved.  
(<http://www.sensorsportal.com>)



International Frequency Sensor Association (IFSA) Publishing

Jacob Y. Wong, Roy L. Anderson

## Non-Dispersive Infrared Gas Measurement



Formats: printable pdf (Acrobat) and print (hardcover), 120 pages

ISBN: 978-84-615-9732-1,  
e-ISBN: 978-84-615-9512-9

Written by experts in the field, the *Non-Dispersive Infrared Gas Measurement* begins with a brief survey of various gas measurement techniques and continues with fundamental aspects and cutting-edge progress in NDIR gas sensors in their historical development.

- It addresses various fields, including:
- Interactive and non-interactive gas sensors
- Non-dispersive infrared gas sensors' components
- Single- and Double beam designs
- Historical background and today's of NDIR gas measurements

Providing sufficient background information and details, the book *Non-Dispersive Infrared Gas Measurement* is an excellent resource for advanced level undergraduate and graduate students as well as researchers, instrumentation engineers, applied physicists, chemists, material scientists in gas, chemical, biological, and medical sensors to have a comprehensive understanding of the development of non-dispersive infrared gas sensors and the trends for the future investigation.

[http://sensorsportal.com/HTML/BOOKSTORE/NDIR\\_Gas\\_Measurement.htm](http://sensorsportal.com/HTML/BOOKSTORE/NDIR_Gas_Measurement.htm)